Temperature Dependent Interaction Energies among X (=Ru, Rh) Impurities in Pd-Rich PdX Alloys

M. Asato, C. Liu, N. Fujima, T. Hoshino, Y. Chen, T. Mohri

Abstract—We study the temperature dependence of the interaction energies (IEs) of X (=Ru, Rh) impurities in Pd, due to the Fermi-Dirac (FD) distribution and the thermal vibration effect by the Debye-Grüneisen model. The n-body (n=2~4) IEs among X impurities in Pd, being used to calculate the internal energies in the free energies of the Pd-rich PdX alloys, are determined uniquely and successively from the lower-order to higher-order, by the full-potential Korringa-Kohn-Rostoker Green's function method (FPKKR), combined with the generalized gradient approximation in the density functional theory. We found that the temperature dependence of IEs due to the FD distribution, being usually neglected, is very important to reproduce the X-concentration dependence of the observed solvus temperatures of the Pd-rich PdX (X=Ru, Rh) alloys.

Keywords—Full-potential KKR-Green's function method, Fermi-Dirac distribution, GGA, phase diagram of Pd-rich PdX (X=Ru, Rh) alloys, thermal vibration effect.

I. INTRODUCTION

WE have been studying the dependence of the solvus temperature (T_{solvus}) on the X-concentration for the Pd-rich PdX (X=Ru, Rh) alloys [1], by the free energy calculations based on the cluster variation method within the tetrahedron approximation (CVMT) for the configurational entropy [2], [3]. The internal energies in the free energies of Pd-rich PdX alloys are expanded by use of the real space cluster expansion (RSCE) with the interaction energies (IEs) among X impurities in Pd, which are calculated using the full-potential Korringa-Kohn-Rostoker (FPKKR) Green's function method for perfect and impurity systems (Pd-host and X_n in Pd, n=1~4) [2]-[8].

It is experimentally revealed that the temperature region of the observed T_{solvus} is very wide (from 1000 K to 1600 K) for $Pd_{1-c}Ru_c$ ($0.03 \leq c \leq 0.12$) alloys, while very narrow (from 820 K to 860 K) for the $Pd_{1-c}Rh_c$ ($0.09 \leq c \leq 0.12$) alloys [1]. It is also noted that the observed T_{solvus} is very high. Therefore, it may be important to include the temperature effects into the calculation procedures mentioned above. Moreover, we very

recently found that the 2-body IE at the 9th-nearest neighbor (nn) is considerably large for the Ru impurities in Pd [3]. Thus, we have studied the distance dependence of the 2-body IEs up to the 20th-nn, including not only the local lattice relaxation effect for the 1st-nn 2-body X-X IE, existing even at T=0 K, but also the thermal lattice vibration effect [3], [9], and the electron excitation effect due to the Fermi-Dirac (FD) distribution [3], [10]. We found that the temperature (T_{FD}) dependence of the electron excitation effect due to FD distribution, being usually neglected, is very important to reproduce the observed T_{solvus} of the Pd-rich PdX (X=Ru, Rh) alloys. The purpose of the present paper is to clarify the temperature dependence of the IEs among X impurities in Pd-rich PdX alloys, due to the FD distribution and the thermal vibration by the Debye-Grüneisen model.

In Section II, we discuss briefly the calculation procedures of the present FPKKR with the electron excitation effect due to the FD distribution, the thermal vibration by the Debye-Grüneisen model, and the free energy calculations based on the CVMT for the configurational entropy. In Section III, we show how the T_{FD} dependence for the IEs is important to reproduce the X-concentration dependence of the observed T_{solvus} of the Pd-rich $Pd_{1-c}X_c$ (X=Ru, Rh) alloys. Section IV summarizes the main results of the present paper.

II. CALCULATION METHOD

We describe briefly the calculation procedures for the FPKKR with the electron excitation effect due to the FD distribution (in A), the thermal vibration effect by the Debye-Grüneisen model (in B), and the free energy calculations based on the CVMT for the configurational entropy (in C), because the details of the calculation procedures are written in [3], [9]-[15].

A. FPKKR Calculations for Total Energies of $Pd_{1-c}X_c$ (X=Ru, Rh) Alloys

The present ab-initio calculations are based on the density functional theory (DFT) in the generalized gradient approximation (GGA) [11], [12]. In order to solve the Kohn-Sham equations, we use a multiple scattering theory in the form of the KKR Green's function method for the full-potentials (FP). We use the screened version of FPKKR band calculations for Pd host, which significantly simplifies the numerical calculations by introducing the short-range structural Green's functions [13], [14]. In order to simplify the total energy calculations in the GGA formalism, we use the electronic densities obtained self-consistently by the local spin density approximation in the DFT. The accuracy of the present GGA calculations was discussed in [11], [12]. The RSCE for

M. Asato is with the National Institute of Technology, Niihama College, Niihama, Ehime 792-0811, JAPAN (corresponding author, phone: +81 897-37-7808; e-mail: asato@sci.niihama-nct.ac.jp).

C. Liu, is with the National Institute for Materials Science, Tsukuba 305-0047, Japan.

N. Fujima is with the Graduate School of Engineering, Shizuoka University, Hamamatsu 432-8561, Japan.

T. Hoshino is with the Faculty of Engineering, Shizuoka University, Hamamatsu 432-8561, Japan.

Y. Chen is with the Graduate School of Engineering, Tohoku University, Sendai, 980-8579, Japan.

T. Mohri is with the Institute for Materials Research, Tohoku University, Sendai, 980-8577, Japan.

World Academy of Science, Engineering and Technology
International Journal of Materials and Metallurgical Engineering
Vol:12, No:3, 2018

the internal energies in the free energies of the Pd-rich PdX (X=Ru, Rh) alloys are described in [2]-[8]. The characteristic features of the RSCE is that the IEs among X impurities in Pd-rich PdX alloys are successively determined from the lower-order to high-order (for the first time from Pd-host, and one-body, two-body,···) and independent of the concentration [6], [8].

As discussed in [3], in order to calculate the dependence of the T_{solvus} on the X-concentration for the $Pd_{1-c}X_c$ alloys, we must first calculate the total energy difference between the disordered and segregated states. The total energies (per tetrahedron basic cluster) of the disordered and segregated states, within the CVMT approximation, are written as follows:

$$E_{\text{dis}} = 2\sum_{ijkl} E_{ijkl}\omega_{ijkl} \tag{1}$$

where $i, j, k,$ and l distinguish Pd or X, E_{ijkl} is the total energy (per tetrahedron basic cluster), and ω_{ijkl} is the cluster probability. E_{ijkl} is calculated using the IEs up to the 4-body, obtained in the RSCE. It is noted that the segregated state corresponds to the case of $\omega_{\text{RhRhRhRh}} + \omega_{\text{PdPdPdPd}} = 1$ (Rh-concentration $= \omega_{\text{RhRhRhRl}}$, Pd-concentration $= \omega_{\text{PdPdPdPd}}$), as discussed in Appendix 2 in [3].

In the present study, we calculate the T_{FD} dependence of the IEs due to the FD distribution. As shown in [10], the introduction of the FD distribution into the *ab-initio* Green's function calculations is very useful to simplify the ground state calculations. Based on a contour integration in the complex energy plane, we evaluate the residues at a few Matsubara frequencies, while the remaining integral was analyzed by the Sommerfeld expansion. The imaginary part (δ) in the complex energy plane is related to the T_{FD} of the FD distribution ($\delta = \pi k T_{\text{FD}}$). The total energy is calculated by the grand canonical potential for which a simple formula is given in [10].

In the present study, we also evaluate the local lattice distortion effect for the 1st-*nn* 2-body X-X IE in Pd [3], [15]-[19]. It is noted that the local lattice distortion energy for the 1st-*nn* X-X IE is defined as the difference between the local lattice distortion energies of the two states: (i) the final state where two impurities are located at the 1st-*nn* sites, and (ii) the initial one where both impurities are infinitely apart [16]. The positions of the displaced atoms are determined by the condition of the Hellman-Feynman force=0. The detailed discussion for the local lattice distortion is written in [15].

B. Vibrational Free Energies

In addition to the local lattice distortion effect due to the difference in atomic size, existing even at T=0 K, the effect of the lattice softening due to the thermal vibration at finite temperatures is considered in the present study. The vibrational free energy for the lattice softening is calculated using the Debye-Grüneisen model which is based on the quasi-harmonic approximation. By following [9], the vibrational free energy

($F_{\text{vib}}^{(n)}(a,T)$) of each phase ($n$) in the basic cluster $Pd_{4-n}X_n$ (n=0~4) used in the CVMT (see Fig. 2 in [2]; H=Pd, I=X) is written as follows:

$$F_{\text{vib}}^{(n)}(a,T) = E_{\text{vib}}^{(n)}(a,T) - TS_{\text{vib}}^{(n)}(a,T) \tag{2}$$

where $E_{\text{vib}}^{(n)}(a,T)$ is a vibrational internal energy and $S_{\text{vib}}^{(n)}(a,T)$ is a vibrational entropy, depending on the lattice parameter (a), temperature (T), and the phase (n) specified by the basic cluster ($Pd_{4-n}X_n$), as discussed in [3] and [9].

C. Free Energy Differences between Disordered and Segregated States and Solvus Temperatures

In the present study, we calculate the free energy difference (3) between the disordered and segregated states,

$$\Delta F(a,T) = \Delta E(a,T) - TS_{\text{con}}(a,T) \tag{3}$$

$$\Delta E(a,T) = E_{\text{dis}}(a,T) - E_{\text{seg}}(a,T) \tag{4}$$

where $E_{\text{dis}}(a, T)$ and $E_{\text{seg}}(a, T)$ are the internal energies corresponding to the disordered and segregated states, respectively, depending on the lattice parameter (a) and temperature (T), and include the contributions from the electron excitation due to the FD distribution and the thermal vibration effect (2) based on the Debye-Grüneisen model. The $S_{\text{con}}(a, T)$ is the configurational entropy calculated by CVMT. The $S_{\text{con}}(a,T)$ and $\Delta E(a, T)$ are expressed by the cluster probabilities {ω_{ijkl}} of the tetrahedron, where $i, j, k,$ and l distinguish Pd or X. Thus, by minimizing the free energy difference (3) with respect to the cluster probabilities {ω_{ijkl}}, we can determine the cluster probabilities in the equilibrium state. The X-concentration limit to a given temperature (T_{solvus}) is calculated by using the calculated values for {ω_{ijkl}}. The calculation procedure for the minimization of $\Delta F(a, T)$ is described in Appendix 2 in [3].

III. CALCULATED RESULTS FOR INTERACTION ENERGIES AND SOLVUS TEMPERATURES OF PD-RICH PDX ALLOYS

Fig. 1 shows the calculated results for the distance dependence (the 1~20th-*nn*) of X-X (X=Ru, Rh) IEs in Pd. The positive IE means a repulsion, while the negative IE an attraction. It is found that the 2-body interaction is very long-range for Ru impurities in Pd and may be important up to the 10th-*nn*. The repulsive 2-body IEs at the 2nd-, 4th-, and 9th-*nn*s are considerably large. For Rh impurities in Pd, the repulsive 2-body IEs at the 2nd-, 9th-*nn*s are also large, although the attractive 2-body IE at the 1st-*nn* is dominant. However, the 2~4 body IEs among X impurities, only up to the tetrahedron formed by the 1st-*nn* pairs, can be included in the present CVMT. Thus, as the first approximation we renormalize the 1st-*nn* IE as follows [2], [3],

Open Science Index, Materials and Materials and Metallurgical Engineering Vol:12, No:3, 2018 publications.waset.org/10008666.pdf

International Scholarly and Scientific Research & Innovation 12(3) 2018   125   ISNI:000000091950263

World Academy of Science, Engineering and Technology
International Journal of Materials and Metallurgical Engineering
Vol:12, No:3, 2018

$$\Delta \widetilde{E}_1^{2-\text{body}} = \Delta E_1^{2-\text{body}} + \frac{6}{12} \Delta E_2^{2-\text{body}} + \frac{24}{12} \Delta E_3^{2-\text{body}} +$$

$$\cdots + \frac{24}{12} \Delta E_{10}^{2-\text{body}} \tag{5}$$

where the coefficient in the *n*th-*nn* term is the ratio of the coordination numbers of the *n*th-*nn* shell to that of the 1st-*nn* shell. It is noted that the sum total of the long-range 2-body IEs is maintained in the renormalized 1st-*nn* IE. In the present paper, the CVMT calculations with the 1st-*nn* IE renormalized by the IEs up to the 10th-*nn* are written as CVMT10. The thermal vibration effect is also included in the renormalized 1st-*nn* IE, as discussed in Appendix 1 in [3].

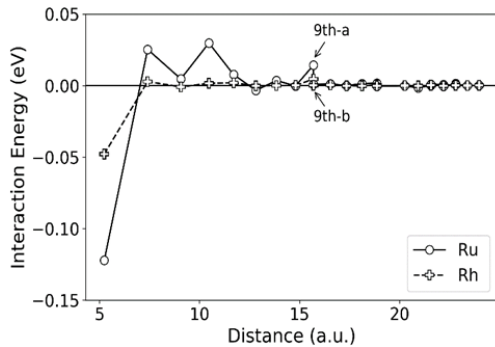Fig. 1 Calculated results for the distance dependence (1~20th-*nn*) of X-X (X=Ru, Rh) IEs in Pd at the lattice parameter of 7.40 a.u., with the FD distribution at T_{FD} =800 K. There are two nonequivalent sites for the 9th-, 13th-, 16th-, 17th-, and 18th-*nn* sites. The 9th-a and 9th-b *nn* sites are (1.5, 1.5, 0) and (2, 0.5, 0.5) in the unit of the lattice parameter (7.40 a.u.), respectively. See the text for details

Fig. 2 shows the T_{FD} dependence for the 2-body IEs up to the 10th-*nn* for (a) Ru-Ru IEs and (b) Rh-Rh IEs. We found that the repulsive interaction (positive value) at the 2nd-*nn* becomes weak (less repulsive) with the increasing T_{FD}. This means that the temperature effect of the electron excitation due to the FD distribution attractively works for the 2-body IEs. We also found that the T_{FD} dependence for X=Ru is much larger than that for X=Rh. The 2nd-*nn* IE changes from 0.0211 eV (T_{FD}=1000K) to 0.0085 eV (T_{FD}=1600 K), for the temperature region (1000~1600 K) of the observed T_{solvus} of the $Pd_{1-c}Ru_c$ ($0.03 \leq c \leq 0.12$) alloys, as shown in Fig. 2 (a). On the other hand, the 2-body IEs are almost unchanged for the temperature region (820~860 K) of the observed T_{solvus} of the $Pd_{1-c}Rh_c$ ($0.09 \leq c \leq 0.12$) alloys, as shown in Fig. 2 (b). For example, the energy difference between the 2nd-*nn* IEs (0.0036 and 0.0030 eV) at T_{FD}=800 and 900 K is as small as 0.0006 eV, although the energy difference between the 2nd-*nn* IEs (0.0093 and 0.0030 eV) at T_{FD}=200 and 900 K becomes as large as 0.0063 eV. The temperature dependences of the thermal vibration effect for the renormalized 1st-*nn* 2-body IEs of X impurities in Pd, by the Debye-Grüneisen model, are listed in Tables I (for X=Ru) and II (for X=Rh). The thermal vibration effect for the renormalized 1st-*nn* IE is taken into account in the present calculations, as discussed in Section II and [3], [9]. It is found that the temperature effect due to the thermal vibration attractively works for the 2-body X-X IEs in the Pd-rich PdX

alloys, as well as the FD distribution, although it is smaller compared to that due to the FD distribution.
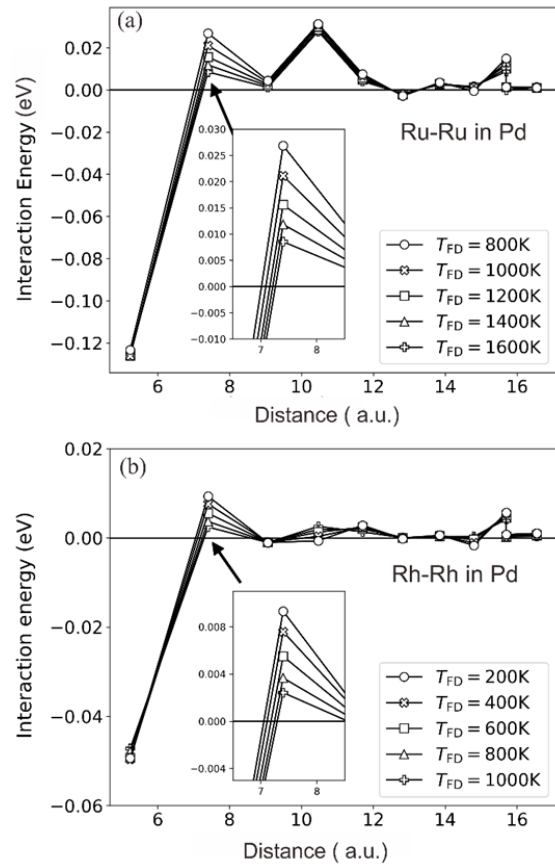

Fig. 2 Calculated results for the T_{FD} dependence of the 2-body IEs (1st~10th) of X-X (X=Ru, Rh) in Pd, at the lattice parameter of 7.40 a.u. The Ru-Ru IEs are shown in (a), while the Rh-Rh IEs in (b). See the text for details

TABLE I
CALCULATED RESULTS (IN eV) FOR THE RENORMALIZED 1ST-*NN* IES WITH THE THERMAL VIBRATION AT T_{vib} = 800, 1200, AND 1600 K. THESE CALCULATIONS WERE EXECUTED WITH THE FD DISTRIBUTION AT T_{FD} = 800, 1200, AND 1600 K, RESPECTIVELY

T_{FD}	renormalized 1st-nn IEs (eV)		
	T_{vib}=800 K	1200 K	1600 K
800K	-0.0662	-0.0681	-0.0705
1200K	-0.0825	-0.0833	-0.0841
1600K	-0.0987	-0.0993	-0.1000

TABLE II
CALCULATED RESULTS (IN eV) FOR THE RENORMALIZED RH-RH 1ST-*NN* IES WITH THE THERMAL LATTICE VIBRATION AT T_{vib} = 600, 800, 1000 K. THE T_{FD} IS FIXED AT 800 K

T_{FD}	renormalized 1st-nn IEs (eV)		
	T_{vib}=600 K	800 K	1000 K
800K	-0.0445	-0.0446	-0.0449

In the present study, we also took into account the local lattice distortion effect for the 1st-*nn* 2-body IE. The calculated lattice distortion energies (negative values) for the 1st-*nn* Ru-Ru IEs at *a*=7.5 and 7.6 a.u., with the FD distribution at

World Academy of Science, Engineering and Technology
International Journal of Materials and Metallurgical Engineering
Vol:12, No:3, 2018

T_{FD}=800, 1000, 1200, 1400 and 1600 K, are listed in Table III. The calculated results for the 1st-nn Rh-Rh IEs at a=7.5 and 7.6 a.u., with the FD distribution at T_{FD}=800 K, are -0.0123 and -0.0125 eV, respectively. It is noted that the local lattice relaxation effect also works attractively for the 1st-nn X-X interaction and that both the dependences on a and on T_{FD} both are very small. In the following calculations for T_{solvus}, the lattice distortion energies for the equilibrium lattice parameters corresponding to the given temperatures (T=800, 1000, 1200, 1400, 1600 K), are estimated by interpolating or extrapolating the two values at 7.5 and 7.6 a.u.

TABLE III
CALCULATED RESULTS (IN EV) FOR THE LOCAL LATTICE DISTORTION
ENERGIES FOR THE 1ST-NN RU-RU IES IN PD. THESE CALCULATIONS WERE
EXECUTED AT TWO LATTICE PARAMETERS (a=7.5, 7.6 A.U.) WITH FD
DISTRIBUTION AT T_{FD} = 800, 1000, 1200, 1400 AND 1600 K, RESPECTIVELY

a(a.u.)	local lattice relaxation energies (eV)				
	T_{FD}=800 K	1000 K	1200 K	1400 K	1600 K
7.5	-0.0336	-0.0340	-0.0342	-0.0344	-0.0346
7.6	-0.0346	-0.0349	-0.0353	-0.0357	-0.0361

We now discuss the calculated results for the X-concentration dependence of the observed T_{solvus} of the Pd$_{1-c}$X$_c$ (X=Ru, Rh) alloys, using the temperature dependent IEs due to the FD distribution and the thermal vibration effect. For the T_{solvus} of the Pd$_{1-c}$Ru$_c$ alloys, we found that the T_{FD} dependence (1000~1600 K) is very important to reproduce the Ru-concentration dependence of T_{solvus} of the Pd$_{1-c}$Ru$_c$ alloys, as shown in Fig. 3 (a). It is obvious that the experimental results for the T_{solvus} are never reproduced by the *ab-initio* calculations without the T_{FD} dependence for IEs. In the present calculations, the observed T_{solvus} to a given Ru-concentration (shown by a vertical dotted line) should agree with the calculated result (○) obtained by using T_{FD}=T_{solvus}. We then compared the calculated results (○) with the experimental results (×) for the T_{solvus} to given Ru-concentrations (shown by vertical dotted lines). For the observed T_{solvus}=1000 K, 1200 K and 1400 K, corresponding to Ru-concentration limits =2.7%, 4.4 %, and 7.8%, the present calculations with T_{FD}=T_{solvus} agree very well with the observed T_{solvus}=1000 K, 1200 K and 1400 K. For the observed T_{solvus}=1600 K, corresponding to Ru-concentration limit=12%, the present calculation overestimates the experimental result by ~200 K. We already discussed that these discrepancies may be mainly due to the insufficient renormalization for the long-range 2-body IEs [3]. According to the Monte-Carlo simulations by Schweika [20], the overestimation of the T_{solvus} due to the insufficient renormalization becomes larger and larger with the increasing concentration of minor element X, for the alloys with the competitive 2-body IEs (the strongly attractive IE at the 1st-nn and the considerably repulsive IE at the 2nd-nn), being similar to the present Pd-rich PdX alloys. It is shown in [3] that the calculations based on the cluster variation method within the tetrahedron-octahedron approximation (CVMTO), in which the 1st- and 2nd-nn IEs are treated exactly, may correct the high discrepancies in the high Ru-concentrations (~12%), if the 2nd-nn IE (repulsion) is renormalized by including the 4th-nn
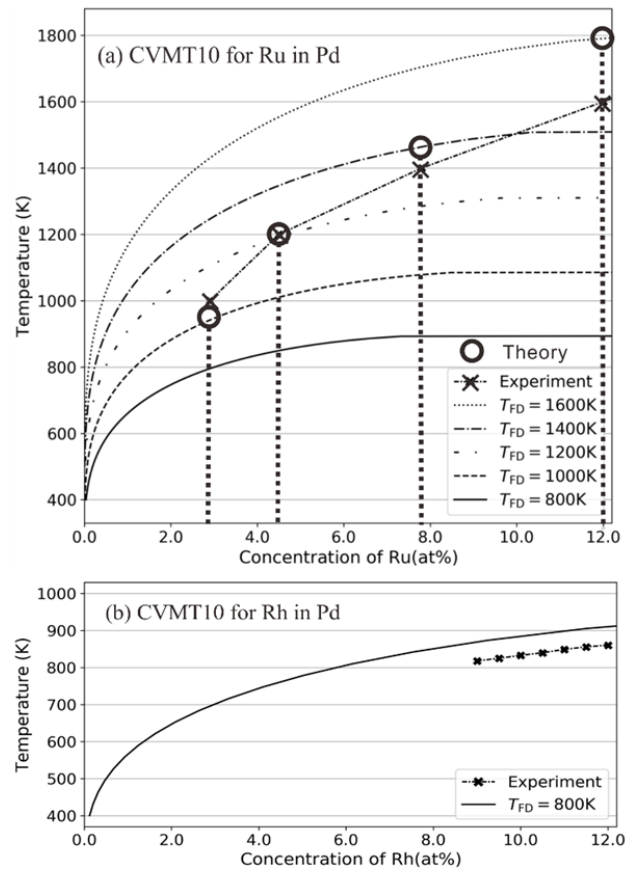
IE (large repulsion at high temperatures).

Fig. 3 Calculated results for the X-concentration (X=Ru, Rh) dependence of Solvus temperatures of (a) Pd$_{1-c}$Ru$_c$ and (b) Pd$_{1-c}$Rh$_c$ alloys. See the text for details

For the observed T_{solvus} (820~860 K) of the Pd$_{1-c}$Rh$_c$ alloys in Fig. 3 (b), the T_{FD} is fixed at 800 K because the IEs are almost unchanged from 800 to 900 K, as mentioned before. We found that the free energy calculations with T_{FD}=800 K, based on the CVMT10 for the configurational entropy, reproduce (within the error of ~50 K) the Rh-concentration dependence of the observed T_{solvus} of the Pd$_{1-c}$Rh$_c$ alloys, as shown in Fig. 3 (b). It is also found that the small discrepancies between the CVMT10 calculation and experimental results may be reduced from ~50 K to ~20 K, by the free energy calculations based on the cluster variation method within the CVMTO, treating the 1st- and 2nd-nn IEs exactly. The detailed results for the Pd$_{1-c}$Rh$_c$ alloys will be published in [19].

IV. CONCLUSION

We firstly presented the ab-initio calculations for the temperature dependence for the IEs among X (=Ru, Rh) impurities in Pd, due to the FD distribution and the thermal vibration by the Debye-Grüneisen model. We found that the electron excitation effect due to the FD distribution, being usually neglected in the *ab-initio* calculations, is significantly large for the IEs among X impurities in the Pd-rich PdX (X=Ru, Rh) alloys.

World Academy of Science, Engineering and Technology
International Journal of Materials and Metallurgical Engineering
Vol:12, No:3, 2018

We secondly showed that the CVMT10 calculation results for the T_{solvus} of the Pd-rich PdX (X=Ru, Rh) alloy, in which the 1st-nn IE is renormalized by including the 2nd~10th-nn IEs, agree fairy well with the experimental results, although the discrepancies between the CVMT10 calculation and experimental results become significant for the high Ru-concentration (8~12%) of the Pd_{1-c} Ru_c alloys, as shown in Fig. 3 (a). We also discussed that these discrepancies are mainly due to the insufficient renormalization for the long-range 2-body IEs in (5), and that the free energy calculations based on the CVMTO for the configurational entropy, in which the 2nd-nn repulsive IE can be treated independently from the 1st-nn attractive IE, may correct the high discrepancies in the high Ru-concentration (8~12%), if the 2nd-nn IE is renormalized by the 4th-nn IE (considerably strong repulsion) [3]. The CVM calculations with the large basic cluster including up to the 4th-nn IE is strongly requested to quantitatively determine the phase diagrams of the long-range interaction systems such as the Pd-rich PdRu alloys.

REFERENCES

[1] T. B. Massalski, H. Okamoto, P. R. Subramanian, and L. Kacprazak: *Binary Alloys Phase Diagrams*, 2nd. ed., (ASM International, New York 1990.

[2] M. Asato, T. Mizuno, T. Hoshino, and H.Sawada, Mater. Trans. 42 (2001), 2216-2224.

[3] C. Liu, M. Asato, N. Fujima, T. Hoshino, Y. Chen, and T. Mohri, to be published to Mater. Trans. 59 (2018).

[4] T. Hoshino, R. Zeller, and P. H. Dederichs, Phys. Rev. B70 (2004), 094118(1-7).

[5] F. Nakamura, T. Hoshino, S. Tanaka, K. Hirose, S. Hirosawa, and T. Sato, Trans. Mat. Res. Soc. Japan 30 (2005), 873-876.

[6] T. Hoshino, M. Asato, N. Fujima, Intermetallic 14 (2006), 908-912.

[7] M. Asato, H. Takahashi, T. Inagaki, N. Fujima, R. Tamura, and T. Hoshino, Mater. Tran. 48 (2007), 1711-1716.

[8] T. Hoshino, M. Asato, and N. Fujima, J. Alloys. Compd. 504 (2010), S534-S537.

[9] T. Mohri and Y. Chen, *J. Alloys. Compd.*383 (2004), 23-31.

[10] K. Wildberger, P. Lang, R. Zeller, and P. H. Dederichs, Phys. Rev. B 52 (1995), 11502-11508.

[11] M. Asato, A.Settles, T. Hoshino, T. Asada, S. Blugel, R. Zeller, and P. H. Dederichs, Phys. Rev. B 60 (1999), 5202-5210.

[12] T. Hoshino, M. Asato, T. Mizuno, and H. Fukushima, Mater. Trans. 42 (2001), 2206-2215.

[13] R. Zeller, Phys. Rev. B55 (1997), 9400-9408.

[14] R. Zeller, M. Asato, T. Hoshino, J. Zalbloudil, P. Weinberger, and P. H. Dederichs: Philos. Mag. B78 (1998), 417-422.

[15] N. Papanikolaou, R. Zeller, P. H. Dederichs, and N. Stefano, Phys. Rev. B 55 (1997), 4157-4167.

[16] T. Hoshino, N. Papanikolaou, R. Zeller, P.H. Dederichs, M. Asato, and N. Stefanou, Comput. Mater. Sci. 14 (1999), 56-61.

[17] M. Asato, C. Liu, K. Kawakami, N. Fujima, and T. Hoshino, Mater. Tran. 55 (2014), 1248-1256.

[18] C. Liu, M. Asato, N. Fujima, and T. Hoshino, Physics Procedia 75 (2015), 1088-1095.

[19] C. Liu, M. Asato, N. Fujima, T. Hoshino, Y. Chen, and T. Mohri, submitted to Mater. Trans.

[20] W. Schweika, Disordered Alloys, (SpringerTracts in Modern Physics 141, Springer 1998), pp.51-54.